Original scientific paper
UDK: 674.23.032.475.4:624.042]:684.4.07

FEM ANALYSIS OF DEFORMATIONS AND STRESSES OF UPHOLSTERED FURNITURE SKELETON MADE OF SCOTS PINE AND OSB

Nelly Staneva, Yancho Genchev, Desislava Hristodorova

University of Forestry - Sofia, Bulgaria
Faculty of Forest Industry, Department "Furniture Production"
e-mail: nelly_staneva@yahoo.com; dhristodorova@yahoo.com

ABSTRACT

A 3D geometric model of one-seat skeleton for upholstered furniture was created by CAD system. A linear static analysis was carried out with CAE system Autodesk Simulation Mechanical® by the method of finite elements (FEM) simulating the loading of skeleton.

The orthotropic material characteristics of pine solid wood (Pinus sylvestris L.) for the rails and OSB for the side plates are considered in the analysis. Two variants of corner joints in the skeleton (*model A* – staples and PVA; *model B* - staples, PVA and strengthening elements) were considered. FEA was performed with regard to laboratory determined and calculated coefficients of rotational stiffness of used staple corner joints.

As results, the distribution of stresses (von Misses and principal), displacements and equivalent strains in the 3D model of upholstered furniture skeleton with staple corner joints are presented and analysed.

Key words: upholstered furniture skeleton, staple joints, deformation and strength, CAE, FEM

1. INTRODUCTION

The skeleton of upholstered furniture is usually wood and/or wood-based products. Although the wood composites are commonly used in box type furniture, their utilization in the frame type furniture is not widespread. It is recommended that wood composites could be used in the production of the frame type furniture, especially in the upholstered furniture frames, but, in this case, it is important according to material type used that the additional reinforcing details and giving a decision about its place in terms of the strength (Kasal, A. 2006).

There is a limited number of references concerning the deformation and strength behaviour of upholstered frames constructed with structure elements of OSB, although OSB panels are increasingly used in the construction of upholstered furniture frames latterly.

Wang, X. (2007a) investigated a three-seat sofa frame made entirely of 18 mm thick OSB plates. With software SAP 2000 she created 3D linear models by beam finite elements of 3 different constructions of a sofa frame with two types of connections – rigid and semi-rigid and two types of connectors: 1) screws and metal plates; 2) staples and metal plates. Nonlinear static analysis was performed simulating 3 loads: light-, medium- and heavy-service. Wang established the most appropriate configuration of the sofa frame of OSB under investigated loads and concluded that the type of connectors does not change the joint displacements and strength remarkably.

Kasal, A. (2006) investigated the strength properties of glued-dowel joined sofa frames constructed of solid wood and wood based composite materials, by using the finite element method (FEM). Considering wood materials as isotropic, he established that the OSB (18 mm thick) has lowest load bearing capacity. The failure of OSB sofa frame was the pull-out of dowels from the member with some core wood particles attached to the dowel and some splits had occurred at the edge of the butt members in the sofa frames.

Erdil Y., A. Kasal and C. Eckelman (2008) investigated the behaviour of 3-seat upholstered furniture frames constructed with ¾ inch thick OSB (EN 300, 1997) and joining elements - yellow birch dowels and aliphatic resin glue (PVAc), using the simplified methods of structural analysis in the engineering of such frames. They concluded that OSB may be used in construction of upholstered furniture frames to meet specific design loads.

More information concerning the strength characteristics of upholstered furniture joints made of OSB is available:

Erdil, Y., J. Zhang and C. Eckelman (2003) defined the edge and face withdrawal strength and lateral edge holding of staple joints for OSB furniture panel components. The test results showed that the holding strength from the face was at least 50% higher than that from the edge of OSB, and the number of staples was nearly proportional to the lateral holding strength of staples on edge of OSB.

Wang, X. et al. (2007b) and Wang, X. et al. (2007c) investigated T-shape corner gusset-plate joints with staples and with/without PVA glue of details of 18 mm thick OSB panels under static bending, torsion and fatigue load. They concluded that the static bending strength increases by 27% when the reinforcing elements are glued. They established that despite differences in failure modes, both stapled and glued stapled joints had similar static-to-fatigue moment capacity ratios – in the stapled joints, the higher ratios were associated with the staple withdrawal as dominating failure mode. They advise to load the gusset-plate joints with maximum of 48% of their static moment capacity.

Data on strength characteristics of other joints of OSB for upholstered furniture in tension, shear, bending and cyclic loads are given by Erdil Y., A. Kasal and C. Eckelman (2008) in the result of previous researches for dowel joints of different construction elements (front rail to stump, top rail to back post and back post to top rail joints of 4-inch thick OSB), Zhang, J., F. Quin and B. Tackett (2001a), Zhang, J., Y. Erdil and C. Eckelman (2002) for dowel joints; Wang, X. et al. 2007d, Wang, X., A. Salenikovich, and M. Mohammad (2008) for metal-plate connected joints; Zang, J. et al. (2001b) for gusset-plate joints; Dai at al. (2008) for glued face-to face and end-to-face joints.

The literature study revealed a limited number of publications on skeleton studies of upholstered furniture with staple joints made of OSB.

The aim of this study was to define and analyze the displacements and stresses of one-seat skeleton of upholstered furniture with staple joints and side plates of OSB by CAD/CAE using the method of finite elements (FEM).

2. MATERIALS AND METHODS

A 3D model of one-seat upholstered furniture skeleton with length 600 mm, width 680 mm and height 625 mm was created with Autodesk Inventor Pro® (Educational product) – Fig.1. The used rails are with cross section 25x50 mm.

A linear static analysis of 3D modeled skeleton was carried out with CAD/CAE system Autodesk Simulation Mechanical® (Educational product)by the Finite Elements Method (FEM).

The static analysis was performed with plate elements – Fig.1. The generated mesh (Midplane mesh) has 5130 orthotropic finite elements and 37152 DOF. The contacts between the elements of the skeleton were set corresponding to the physical model.

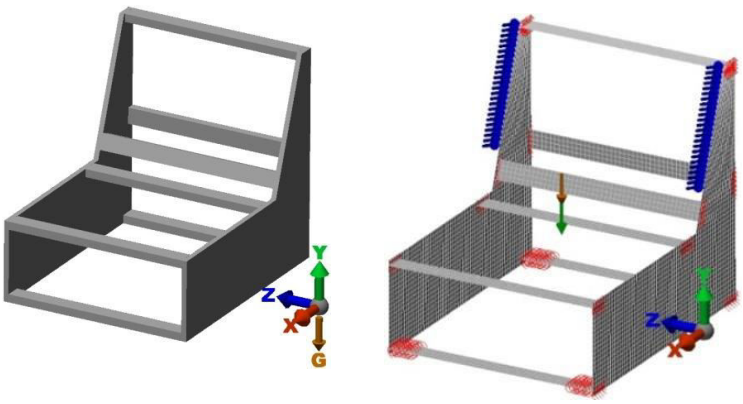

Figure 1. *3D skeleton model and loading*

Orthotropic materials type was used for construction elements of the skeleton:

Scots pine (*Pinus sylvestris L.*) for rails with measured density 435,50 kg/m³ according to BDS EN 323:2001 and elastic characteristics: E_L=12567.10^6 N/m^2, E_R=700.10^6 N/m^2, E_T=545.10^6 N/m^2, G_{LR}=1230.10^6 N/m^2, G_{RT}=800.10^6 N/m^2, G_{LT}=500.10^6 N/m^2, ν_{LR}=0,030, ν_{RT}=0,38, ν_{LT}=0,040 according to Pencik, J. (2014).

Oriented strandboard (OSB), type EGGER OSB2 EN 300 E1 CE, designed for load-bearing structures for use in dry environment, with thickness 16 mm and technical requirements according to BDS EN 13986:2004+A1:2015, were used for side plates.

The physical and mechanical characteristics of the OSB panels are:

Density 595.67 kg/m³, measured according to BDS EN 323:2001;

Modulus of elasticity in bending (major axis) - E_1=3800.10^6 N/m^2;

Modulus of elasticity in bending (minor axis) - E_2=3000.10^6 N/m^2;

Bending strength (major axis) - 16,4.10^6 N/m^2;

Bending strength (major axis) - 8,2.10^6 N/m^2;

Poisson ratios ν_{12}=0,030 according to Thomas, W. (2003) and ν_{21}=0,24, calculated according to Bodig J. and B. Jayne (1982) by the equation:

$$\frac{\nu_{12}}{E_1}=\frac{\nu_{21}}{E_2}, \quad (1)$$

Support boundary conditions were set: bottom front rail – no translation on *y* direction and bottom rear rail no translation on *x*-, *y*- and *z* direction.

In order to simulate semi-rigid connections between rails and side plates of the skeleton, the laboratory determined coefficients of rotational stiffness of the joints, loading under compression (Hristodorova, 2017) were introduced in the nodes of the respective corner joints - case butt joints and end to face butt joints with 2 staples (type M1), PVA glue and with/without additional triangle strengthening detail. For this purpose two FEA models were created and two design scenarios were performed:

Model A: all joints of the skeleton are with staples and PVA glue and rotational stiffness coefficient *c*=732.01 N.m/rad for case butt joints and *c*=507.43 N.m/rad for end to face butt joint (upper rail of the backrest).

Model B: joints with staples, PVA glue and strengthening details of Scots pine for upper rails of the seat (case butt joints) with rotational stiffness coefficient *c*=1900.57 N.m/rad and *c*=1720.88 N.m/rad for upper rail of the backrest (end to face butt joint). The rotational stiffness coefficients of all the rested joints of the skeleton are set as these in *model A*.

The following loads in both FEA models were set - Fig.1:

Seat: heavy-service load F_{seat} = 3x800 N = 2400 N with application point of 100 mm from the upper rear rail, set as a remote force, distributed only between upper rails of the seat, simulating upholstery base made of zig-zag springs;

Backrest: $F_{backrest}$ = 200 N, set as equal nodal forces, distributed on the edges of the two sides of the backrest.

The changed angle γ between the joint shouders at upper front rails of the seat was mesuared with the program Autodesk Simulation Mechanical®.

3. RESULTS AND DISCUSSION

The results for linear displacemets *u*, nodal rotations θ, von Mises stresess $\sigma_{von\ Mises}$, maximum principal stresses σ_1, minimum principal stresses σ_3 and equivalent strains $\varepsilon_{von\ Mises}$, as well as the changed angle γ between the joint shouders at upper front rails of the seat for both *models A* and *B,*are shown in Table 1 and in Fig.2 to Fig 6 for the skeleton and for the side plates of the skeleton, respectively. The visualizations of the deformed model are shown with a scale factor 1% of model size for the skeleton and with a scale factor 100% of model size for the side plates.

In Fig.2 the distribution of resultant displacement is presented. The maximal resultant displacements of 17.12 mm for *model A* and 11.47 mm for *model B* are received in the middle of the upper rails of the seat, on the inside of the rails and are determined mainly by the *y*-displacements (u_y)

– Table 1. The resultant displacement is bigger in the front upper rail than it is in the rear upper rail of the seat for both models – 7,01% for *model A* and 11,47% for *model B*. This is due to the nature of the applied force with application point of 100 mm to the rear upper rail (Genchev, 2017), which coincides with the application of the weight of the discrete model of the skeleton.

Table 1. *Displacements and strains of the skeleton and the skeleton side plates*

Parameters	**Skeleton**		**side plates**	
	model A	*model B*	*model A*	*model B*
u_{res}, *[mm]*	17.12	11.47	0.678	0.229
u_x, *[mm]*	-0.238	-0.199	-0.198	-0.199
u_y, *[mm]*	-17.12	-11.47	-0.146	-0.122
u_z, *[mm]*	0.669	0.986	0.669	0.0986
θ_{res},[°]	6.21	4.865	0.827	0.2325
θ_x, [°]	-4.93	-3.567	-0.767	-0.2026
θ_y, [°]	-0.175	-0.075	-0.175	-0.0749
θ_z, [°]	5.34	4.45	0.426	0.119
$\varepsilon_{von\ Mises}$, [*m/m*]	0.03201	0.015975	0.007204	0.002883
γ, [°]	89.0068	89.7106		

In the side plates the maximum values of the resultant displacement for *model A* are received in the points of the base of the seat where dissolution of the side plates is observed - Fig.2. This is due to the fact that the resultant displacements are determined mainly by *z*-displacements (u_z) and lower by *x*-displacements (u_x).

The maximum values of the resultant displacements for *model B* were located in the upper part of the side plates in the contact field of the side plates with the upper rail of the beckrest, because the resultant displacements are determined mainly by *x*-displacements (u_x) and lower by *y*-displacements (u_y) - Table 1 and Fig.2. A difference of 66,22% between resultant displacements for *model A* and *model B* was established.

The maximal resultant nodal rotations θ_{res}=6.21° for *model A* and θ_{res}=4.865° for *model B* are located in the front upper rails for both models – Fig.3. It was observed that the resultant nodal rotation is bigger in the front upper rail than it is in the rear upper rail of the seat for both models – 22,54% for *model A* and 27,93% for *model B*.

Maximal values of resultant nodal rotation in the side plates are received in the contact field with the front upper rail. For the skeleton model they are determined mainly by rotations about *z*-axis and *x*-axis, and for the side plates they are determined mainly by rotations about *x*-axis and *z*-axis – Table 1. A difference of 71,88% between resultant nodal rotations for *model A* and *model B* was established.

It is obvious that the values of u_{res} and θ_{res} are lower for *model B* then those for *model A,* due to of the additional strengthening detail for upper rails of the seat, and this is more clearly expressed for the side plates. The difference for the side plates is approximately 3,56 times for resultant nodal rotations θ_{res} and approximately 2,96 times for resultant linear displacements u_{res}. Expectedly, the change in the angle γ between the joint shouders at upper front rail of the seat is also minor in the presence of a strengthening elements (*model B*) – Table 1.

The distribution of von Mises stresses, maximum principal and minimum principal stresses is presented in Fig.4, Fig.5 and Fig.6.

The maximal values of von Mises stress $\sigma_{vonMises}$=33,40.10^6 N/m^2 are concentrated in the front upper rail of the seat near the side plates for *model A* and $\sigma_{vonMises}$=30,70.10^6 N/m^2 near the strengthening details for *model B* due to the location of the biggest bending moments – Fig. 4. In the rear rail in the same places for both models, the maximum von Mises stresses are almost twice as low as the ones in the front rail, due to the nature of the force applied on the seat. The same relation is observed also for the values of equivalent strains.

The maximum principal stresses (tension stresses) have maximum values located at the top of the rails near the side plates for *model A* and near the strengthening details for *model B*, and the minimum principal stresses (compression stresses) are located at the underside of the upper seat rail in the same locations - Fig.5 and Fig.6. There is obviously a similar distribution of tension and compression stresses in the rear upper rail, as for both models the difference from the values of front upper rail is approximately twice as small.

Von Misses stresses in the side plates have maximum values in the front upper rail contact areas of the seat for both models and are significantly lower (almost 2,46 times) for *model B* than those for *model A* – Fig.4.

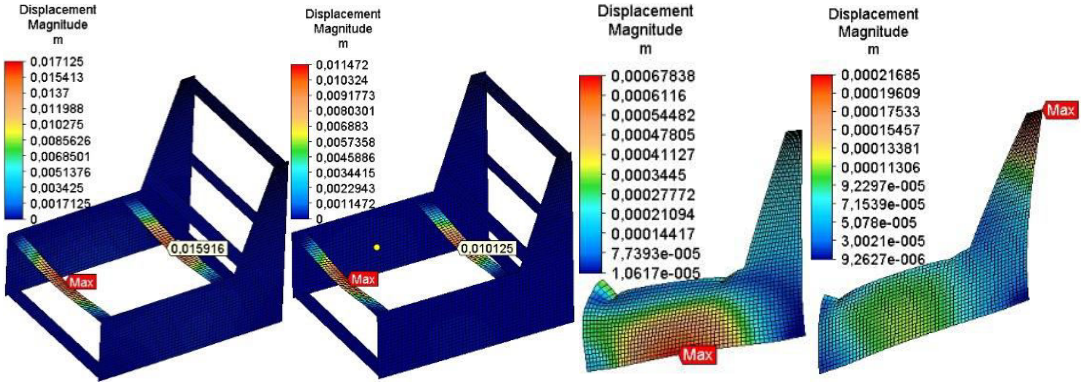

model A *model B* *model A* *model B*

Figure 2. *Distribution of resultant displacements for model A and model B*

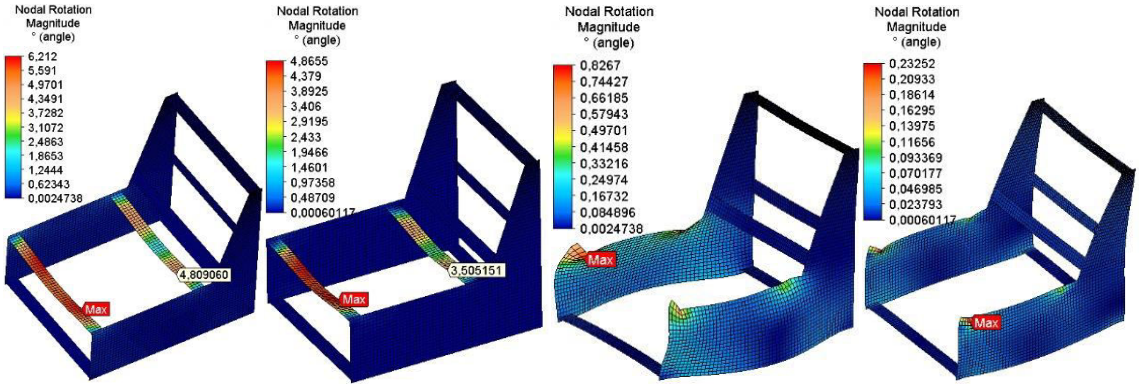

model A *model B* *model A* *model B*

Figure 3. *Distribution of resultant rotational displacements for model A and model B*

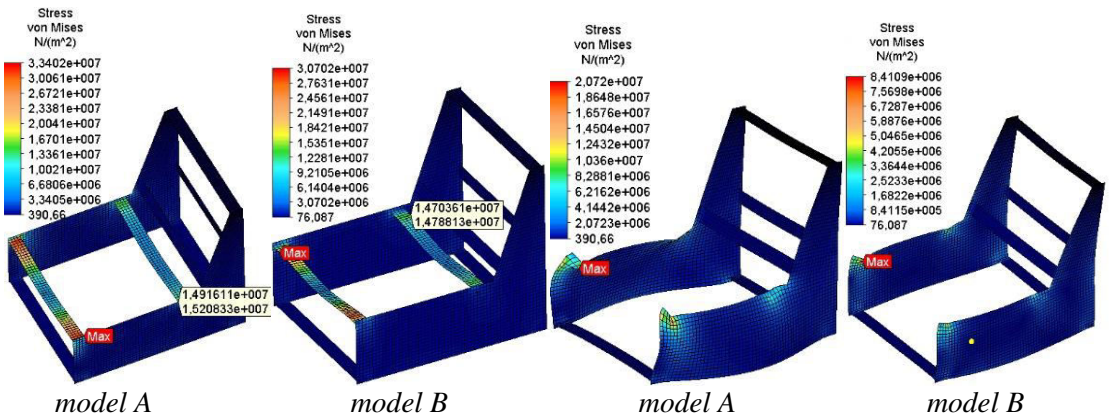

model A *model B* *model A* *model B*

Figure 4. *Distribution of von Mises stresses for model A and model B*

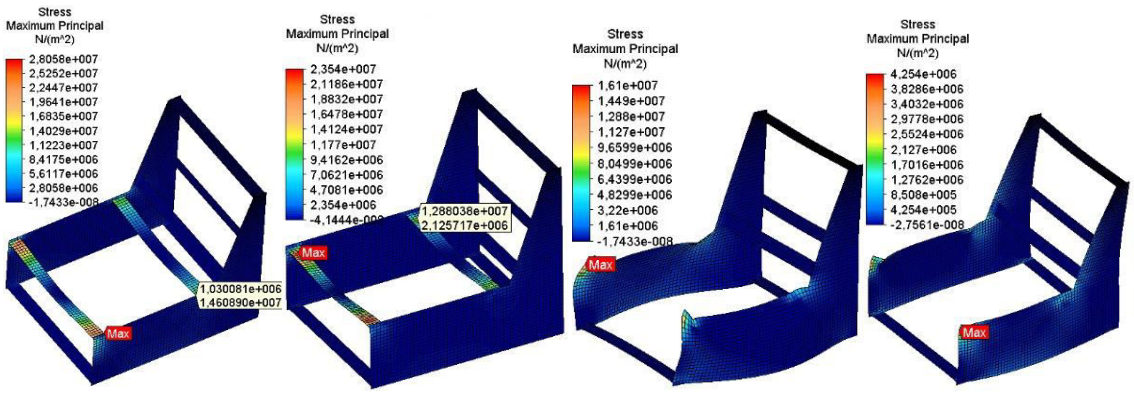

model A *model B* *model A* *model B*

Figure 5. *Distribution of maximum principal stresses for model A and model B*

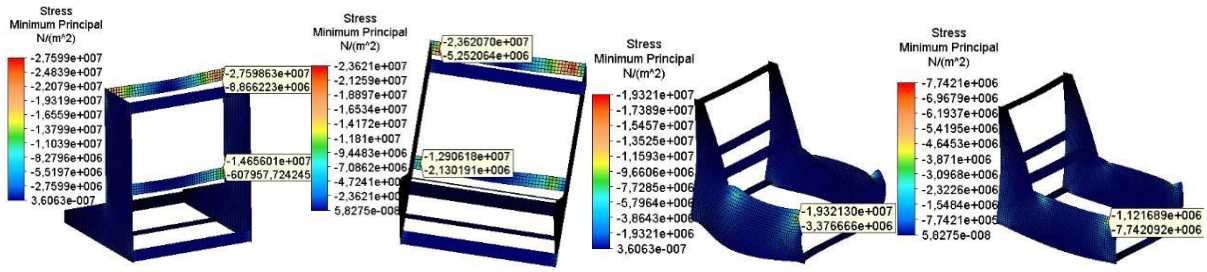

model A *model B* *model A* *model B*

Figure *6.* *Distribution of minimum principal stresses for model A and model B*

Tension stresses reach their maximum in the area of the upper front rail joint and the compression stresses reach their peak in the coupling zones of the front and rear rails on the outside – Fig.5 and Fig.6. There is an obvious and significant decreasing of the tension stresses (almost 3,79 times) and decreasing of the compression stresses (approximately 2,5 times) in the side plates of the skeleton for *model B*. The values of equivalent strain in the side plates for *model B* are 3,5 times as low as those for the *model A* – Table 1.

4. CONCLUSIONS

From the results of this study by FEM with CAE program Autodesk Simulation Mechanical® on the deformations and stresses of one-seat upholstered furniture skeleton with staples and glue joints made of Scots pine and OSB, several conclusions can be derived:

Under heavy-service load on the seat, the critical joints are established – the most loading construction part of the skeleton is the front upper rail where the maximum values for linear displacements, nodal rotations and stresses are received due to the nature of the applied force on the seat.

The deformation behavior in side plates is considerably improved after reinforcement of the front upper rails to side plate joints of the seat - the linear displacements and nodal rotations in the skeleton are reduced approximately by 66.22% and 71.88%, respectively. The change in the angle γ between the shoulders of the front upper rail to side plate of the seat is also minor in the presence of a strengthening element (*model B*). Strength behaviour of the side plates is also impruved - von Mises stresses are reduced by 59.41%, maximum principal stresses by 73,6% and minimum principal stresses by 59,94%.

To improve the deformation and strength behavior of the skeleton side plates, the upper rail on the backrest should be further strengthened in the joints with the side plates.

The reinforcement with solid wood components of the upper rails to side plate joints does not change the displacements and stresses of the skeleton on the whole – it results into a percentage difference between linear displacements of 33.00% and the negligible difference for von Mises stresses by 8,10%.

REFERENCES

[1] Bodig, J. and Jayne, B. (1982): Mechanics of Wood and Wood Composites, Van Nostrand Reinhold Co. Inc., New York.

[2] Dai, L., Zhang, J., Quin, F. (2008): Lateral and Tensile Resistances of Glued Face-to-face Joints in Pine Plywood and Oriented Strandboard, Forest Products J., Vol. 58, No.3, 50-54.

[3] Erdil, Y. Z., Zhang, J., Eckelman, C. A. (2003): Staple Holding Strength of Furniture Frame Joints Constructed of Plywood and Strandboard, Forest Products Journal, 53(1), 70-75.

[4] Erdil, Y., Kasal, A., Eckelman, C. (2008): Theoretical Analysis and Design of Joints in a Representative Sofa Frame Constructed of Plywood and Oriented Strand Board, Forest Products J., Vol. 58, No.7/8, 62-67.

[5] Genchev, Ya. (2017): Special Productions and Wood Products. Production of Upholstered Furniture, Publish house – Univ. of Forestry, Sofia, in print (in Bulgarian).

[6] Hristodorova, D. (2017): Stiffness Coefficients in Joints by Staples of Skeleton Upholstered Furniture, Innovation in Woodworking Industry and Engineering Design (INNO), in print.

[7] Kasal, A. (2006): Determination of the Strength of Various Sofa Frames with Finite Element Analysis, G.U. Journal of Science, vol.19, No.4, 191-203.

[8] Marinova, A. (1996): Methodology of Stress and Strain Furniture Structure Analysis, Proceeding of International Science Conference "Mechanical technology of wood", Sofia, 257-267 (in Bulgarian).

[9] Pěnčík, J. (2014): Modelování Dřeva Pomocí Ortotropního Materiálového Modelu s Kritérii Porušení, Stavební Obzor, No.1–2, 6-7 (in Slovak).

[10] Thomas, W. (2003): Poisson's Ratio of an Oriented Strand Board, Wood Sci. Tehnology, Vol. 37, No.3, 259-268.

[11] Zhang, J., Quin, F., Tackett, B. (2001a): Bending Strength and Stiffness of Two-Pin Dowel Joints Constructed of Wood and Wood Composites, Forest Products Journal, Vol.51, No.2, 29-35.

[12] Zang, J., Lyon, D., Quin, F., Tackett, B. (2001b): Bending Strength of Gusset-Plate Joints Constructed of Wood Composites. Forest Prod. J., Vol.51, No.5, 40-44.

[13] Zhang, J., Erdil, Y., Eckelman, C. (2002): Torsional Strenght of Dowel Joints Constructed of Plywood and Oriented Strandboard, Forest Products Journal, Vol.52, No.10, 89-94.

[14] Wang, X. (2007a): Designing, Modelling and Testing of Joints and Attachment Systems for the Use of OSB in Upholstered Furniture Frames, PhD thesis, University Laval, Quebec, Canada.

[15] Wang, X., Salenikovich, A., Mohammad, M., I. Echavarria, J., Zhang. (2007b): Moment Capacity of Oriented Standboard Gusset-Plate Joints for Upholstered Furniture. Part 1. Static Load. Forest Products Journal, Vol.57, No.7/8, 39-45.

[16] Wang, X., Salenikovich, A., Mohammad, M. J., Zhang. (2007c): Moment Capacity of Oriented Strandboard Gusset-Plate Joints for Upholstered Furniture. Part 2. Fatigue Load. Forest Products Journal, Vol.57, No.7/8, 46-50.

[17] Wang, X., Mohammad, M., Salenikovich, A., Knudson, R. and J. Zhang. (2007d): Static Bending Strength of Metal-Plate Joints Constructed of Oriented Strandboard for Upholstered Furniture Frames. Forest Products Journal, Vol.57, No.11, 52-58.

[18] Wang, X., Salenikovich, A., Mohammad, M. (2008): Out of Plane Static Bending Resistance of Gusset-Plate and Metal-Plated Joints Constructed of Oriented Strandboard for Upholstered Furniture Frames, Forest Products Journal, Vol.58, No.3, 42-49.

[19] www.autodesk.com - Autodesk Simulation Mechanical 2015 – user manual.